FEBS Letters 524 (2002) 204–210 FEBS 26330

Molecular identification and characterisation of the human eag2 potassium channel

M. Ju, D. Wray*

School of Biomedical Sciences, University of Leeds, Leeds LS2 9JT, UK

Received 27 May 2002; revised 25 June 2002; accepted 28 June 2002

First published online 9 July 2002

Edited by Maurice Montal

Abstract We report the molecular cloning from foetal brain of the human potassium channel heag2. The cDNA encodes a protein of 988 amino acids, 73% identical to heag1. Heag2 is expressed in the brain, but is also found in a range of tissues including skeletal muscle. In oocytes, the channel is a non-inactivating outward rectifier, with dependence of activation rate on holding potential. Compared with heag1, the conductance–voltage curve for heag2 was shifted to the left, the voltage sensitivity was less, activation kinetics were different, and the sensitivity to terfenadine was lower. The heag2 channel may have important physiological roles. © 2002 Published by Elsevier Science B.V. on behalf of the Federation of European Biochemical Societies.

Key words: Potassium channel; Human sequence; Outward rectifier K^+ channel

1. Introduction

Potassium channels have key roles in setting membrane potentials, action potential repolarisation and neuronal firing frequency. Consequently they are of vital importance in neurotransmitter and hormonal release, cardiac function, as well as cell cycling and development. These channels are also of great importance as sites of drug action, and are the sites of numerous pathologies such as inherited disorders [1]. Potassium channels comprise several families [2]: two-transmembrane inward rectifiers, four-transmembrane 'twin-pore' channels, and six-transmembrane voltage-dependent channels which include Shaker, KvLQT and ether-a-go-go channel families.

The ether-a-go-go family is characterised by long N- and C-terminal intracellular tails, and is subdivided into eag, elk and erg subfamilies. Within this family, there are now known to be a total of eight genes in rat [2,3]: eag1, eag2, elk1, elk2, elk3, erg1, erg2, erg3. The last member to be cloned, rat eag2, was obtained only recently [4,5].

The erg subfamily [3] is characterised by fast activation, very fast inactivation and inward rectification. Erg channels are widely expressed, including the brain and heart, where cardiac herg1 underlies the I_{Kr} current in the heart and its dysfunction can lead to dangerous arrhythmias. In contrast, the eag subfamily [3] is characterised by outward rectification without inactivation; the (slow) activation kinetics depend on holding potential ('Cole–Moore shift') and extracellular magnesium, while the channel can be blocked by intracellular calcium. The rat eag channels are expressed predominantly in neural tissue; cell cycle-specific expression of eag1 has been demonstrated that may be of great importance in cellular development and tumour growth. Finally, members of the elk subfamily [3] show electrophysiological features like eag (e.g. elk1), or features intermediate between eag and erg (e.g. elk2), though they do not show the Cole–Moore shift [3].

Here, we report the molecular cloning and characterisation of the human eag2 (heag2) channel, and we have compared its functional properties with the previously cloned [6] heag1 channel.

2. Materials and methods

2.1. Cloning of heag2

Predictions for the sequence of the human eag2 channel were obtained using the sequence for the rat eag2 channel [4,5] in BLAST searches against the human genome, together with subsequent analysis using Genscan. From this, primers were designed as follows: 5′-atgccgggggcaagagagggct (sense), 5′-atcctgacatggtatctgggggggtac (antisense) or 5′-ggcaggccagaatccagctggacatg (antisense). These primers were used in PCR reactions using a human foetal brain cDNA library (Clontech), and products were cloned into pGEM-TEasy. Several clones were sequenced (four completely, two partially) to check for sequence consistency.

Heag2 and heag1 clones (the latter in pcDNA3, accession number AJ001366 [6], gift of L. Bernheim) were subcloned into pGEMHE (gift of O. Pongs) for expression in oocytes using *Eco*RI or *Bam*HI respectively, and a Kozak sequence inserted into heag2. After linearisation with *Not*I, capped cRNA was transcribed in vitro using the T7 promoter (Ambion MEGASCRIPT).

2.2. Tissue expression studies

A probe was constructed by PCR using bases 2215–2423 of the heag2 sequence (probe A) in the variable domain, sequenced, and labelled with digoxigenin-11–dUTP using the random primer method (Roche). The probe was used to screen a multiple-tissue Northern blot (MTN, Clontech), and labelling detected by anti-digoxigenin antibody conjugated to alkaline phosphatase, with detection by luminescent light emission using CSPD (Roche).

For RT-PCR expression studies, a multiple-tissue cDNA panel (MTC, Clontech) was used in PCR reactions, using primers designed to amplify bases 2513–3125 of the heag2 sequence using heag2-specific primers. The heag2 clone was used as positive control, and primers against G3PDH were used to check standardisation of cDNA quantities. To check for specificity, Southern blotting was carried out against the RT-PCR products, using a probe spanning the same bases (probe B), prepared by the PCR digoxigenin labelling method with detection as above.

All procedures were carried out according to the manufacturer's instructions.

*Corresponding author. Fax: (44)-113-3434228.
E-mail address: d.wray@leeds.ac.uk (D. Wray).

PII: S0014-5793(02)03055-7

2.3. In vitro translation

The molecular weight of the heag2 protein was obtained using in vitro transcription and translation of heag2 cDNA in pGEMHE. For this, heag2 protein was made in the presence of [^{35}S]methionine using the Promega T7 TNT Quick coupled reticulocyte lysate system with or without canine pancreatic microsomes. Labelled proteins were separated on a 10% SDS–polyacrylamide gel, and exposed to X-ray film.

2.4. Electrophysiology

Xenopus oocytes were injected with 1.5 ng or 7 ng RNA respectively for either heag1 or heag2 in 50 nl, and two-electrode voltage-clamp recordings were made at room temperature (22°C) as previously described [7]. Oocytes in a 50 μl chamber were superfused (1.5 ml/min) with solution containing 2 mM KCl, 115 mM NaCl, 10 mM HEPES, 1.8 mM $CaCl_2$, pH 7.2. Cells were held at −80 mV, and leak and capacity subtraction were carried out using 10 mV hyperpolarising pulses applied at 0.1 Hz. From the same holding potential, test depolarisations (500 ms duration) were applied (0.1 Hz) in order to construct current–voltage (I–V) relationships. For heag2, fits to the current by a Boltzmann function showed deviations, using $I_V = (V-\mathrm{Er})G_{max}/(1+\exp((V_{0.5}-V)/k))$, reversal potential Er = −98.5 mV. This was apparently because of appreciable heag2 currents at the holding potential; instead we fitted to $I_V - I_{-80} - (I_{-80} - I_{-90})(V+80)/10$ (currents I_V, I_{-80}, I_{-90} at voltages V, −80 mV, −90 mV parameterised as above) to correct for heag2 current at the holding potential and the subtraction procedure used; good fits were then obtained. Student's t-test was used to test for significance, and means ± S.E.M. are shown.

3. Results

3.1. Cloning and primary structure

We obtained a heag2 clone containing an open reading frame of 2967 bases, corresponding to a protein of 988 amino acids (Fig. 1), taking the start methionine in the homologous position as in rat eag2 [4,5]. A BLAST search of the human genome with the heag2 sequence showed that the corresponding gene (KCNH5) is located on chromosome 14 at 14q23.1, and the coding sequence comprises 11 exons spanning 338 kb of genomic sequence. The heag2 cDNA sequence was identical to that of the corresponding exons of the genomic sequence, except for one base at position 2577 (counting from the start codon) where the genomic sequence has A instead of G, without however altering the corresponding amino acid. This may be a polymorphism, although we consistently found G in six clones that we sequenced, and also in an EST (accession number U69185). Interestingly, this EST has another base change (G to A at heag2 position 2233), corresponding to a possible mutation/polymorphism A745T in the protein, although G was present in all but one of the clones sequenced in the present study. From comparison with ESTs, the start of the polyA signal is apparently located at base 3200.

The heag2 channel protein has a predicted molecular weight of 112 kDa and isoelectric point of 7.5. In vitro transcription and translation confirmed (Fig. 2C) this molecular weight, where a band of approximately 115 kDa was observed. In the presence of microsomes, where *N*-glycosylation is able to occur, the molecular weight was very similar, implying the absence of marked glycosylation, even though the heag2 sequence displays two consensus sites for *N*-glycosylation at extracellular locations (Fig. 1). Protein bands were also seen at around 105 kDa and 65 kDa, which might correspond to degradation products, or proteins starting from a more downstream methionine.

Heag2 channel protein is 73% identical to heag1, differing

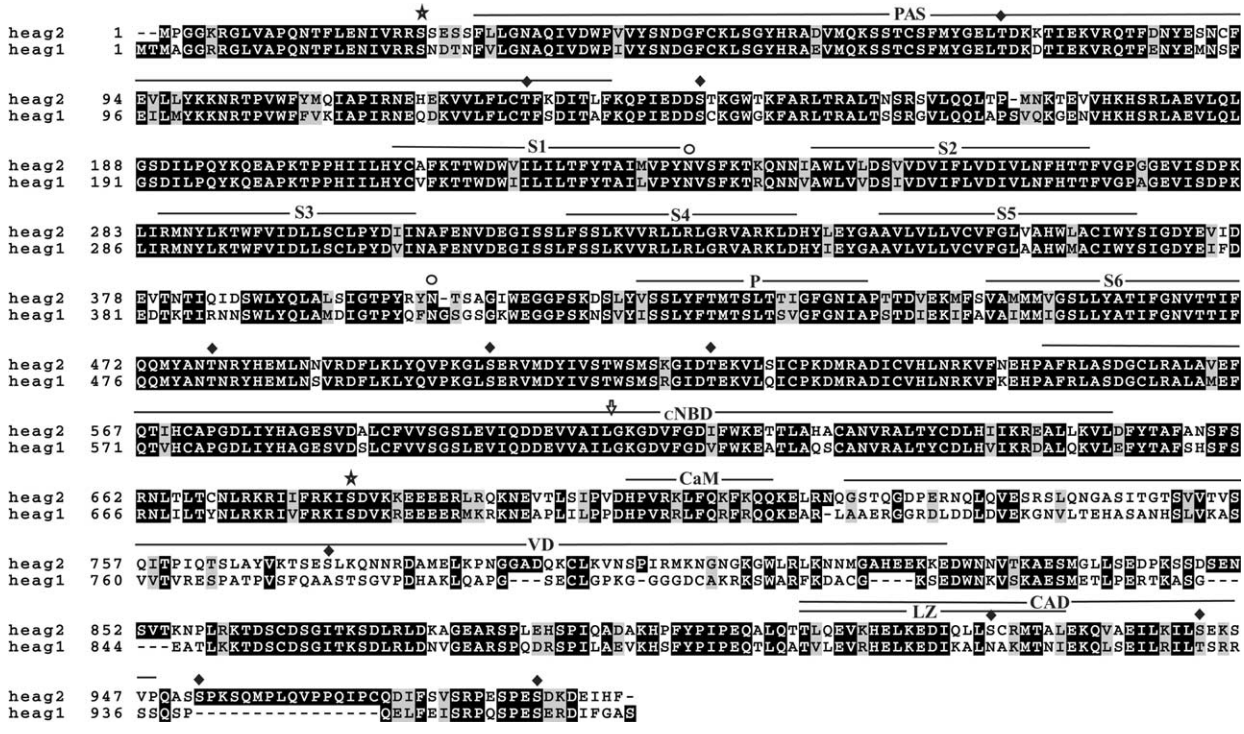

Fig. 1. Sequence alignment of heag1 and heag2 channels. The positions of the characteristic domains are marked. These include the PAS domain, the core channel transmembrane helices, S1–S6 and the pore P region, the cyclic nucleotide binding region, cNBD, the calcium-dependent calmodulin binding region, CaM, the tetramerisation CAD domain, and a leucine zipper region, LZ. A variable domain (VD) between heag1 and heag2 is also shown. For heag2, the intracellular consensus sites for cAMP/cGMP phosphorylation (★) and for protein kinase C phosphorylation (♦) are marked, as are the extracellular consensus sites for *N*-glycosylation (○). The arrow marks the position for alternative splicing; the splice variant terminates four amino acids after the position shown. We have deposited the sequences at GenBank, accession numbers AF472412 and AF493798. The 2233A polymorph was used for expression studies.

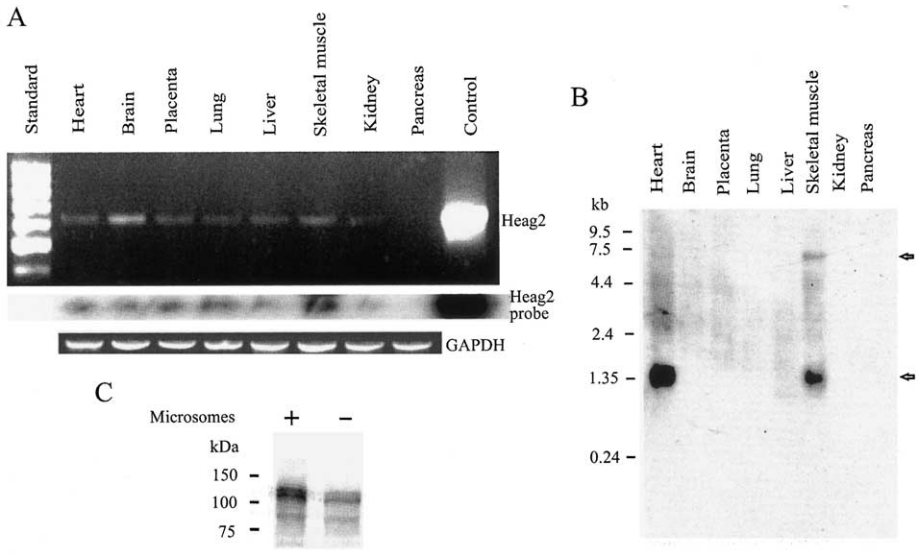

Fig. 2. Expression of heag2: tissue distribution and protein translation. A: RT-PCR was carried out for various human tissues using heag2-specific primers (top) or GAPDH primers (bottom). A control PCR is also shown using heag2 cDNA as template. The figure shows analysis by agarose gel. A Southern blot of the gel was made using a heag2-specific probe (probe B) (middle). B: Northern blot of human RNA for various tissues, using a heag2-specific probe (probe A). The arrows show the positions of the two bands. C: In vitro transcription and translation of heag2 using rabbit reticulocyte, in the presence or absence of microsomes. ^{35}S-labelled protein was analysed by SDS gel.

mainly at a C-terminal region of some 104 amino acids, VD (Fig. 1). In common with other members of the ether-a-go-go family, heag2 possesses conserved domains (PAS, cNBD, CAD domains) characteristic of this family [8–10] (Fig. 1). There is also a calmodulin binding domain [11,12], indicating that heag2 is sensitive to intracellular calcium block, as for rat eag1.

One of the heag2 clones sequenced was a splice variant with exon 10 missing (Fig. 1), resulting in a shorter protein (611 amino acids), truncated within the cNBD region. Its properties were not investigated further here; however, it may be a channel that is non-functional on its own, similar in that respect to the 'Herg$_{USO}$' channel [13], which is also alternatively spliced in the cNBD.

3.2. Heag2 RNA tissue expression

In RT-PCR studies of tissue distribution of heag2 (Fig. 2A), after 30 cycles of PCR the strongest signal was seen predominantly in brain, the next strongest in skeletal muscle, and expression was also detected in heart, placenta, lung, liver, and at low levels in kidney. Continuing the PCR for four further cycles also showed clear signals in kidney and pancreas (data not shown). These general features were confirmed by repeating the analysis on a second, independent MTC panel. There was a similar pattern of localisation in a Southern blot, confirming the specificity of the RT-PCR reactions. In Northern blots (Fig. 2B), RNA transcripts at approximately 1.4 kb and 6.8 kb were observed in heart and skeletal muscle. The smaller-sized transcript may be a splice variant, as previously suggested for rat eag2 [4]. Surprisingly, no transcript was seen in whole brain, reminiscent of a similar situation for rat eag2 [4], where only very weak signals were seen for whole brain in Northern blot, even though other data showed strong expression in various brain regions.

3.3. Functional studies

RNA for heag2 was expressed in oocytes, and voltage-clamp recordings of expressed currents were made. Currents for heag2, like heag1, were non-inactivating, characteristic [4–6,11,14] of eag channels (Fig. 3A,B), and I–V curves for heag1 and heag2 (Fig. 3C,D) showed outward rectification. Heag2 currents activated at more negative potentials than for heag1, as can also be seen from G–V plots (Fig. 3E). There was a leftward shift for heag2 as compared with heag1; furthermore, the voltage sensitivity was less steep for heag2, reflecting less voltage-sensitive transitions to the open state for heag2. More specifically, mean $V_{0.5}$ was -11.4 ± 3.4 mV for heag2 ($n = 17$), significantly different ($P < 0.05$) from the value for heag1 ($+10.1 \pm 1.4$ mV, $n = 20$), while k was 34.7 ± 2.0 mV for heag2, again significantly different ($P < 0.05$) from that for heag1 (17.2 ± 1.2 mV). Plots of activation time (time for 20 to 80% of maximal current) versus test potential are shown in Fig. 3F; it is clear that activation times are significantly slower for heag2 than for heag1.

The activation rate depends on holding potential for both heag2 and heag1 (Fig. 4A,B); activation is faster for more positive holding potentials (Cole–Moore shift). At first glance the heag1 currents shown in Fig. 4B appear to activate more slowly than those for heag2 in Fig. 4A, at least at hyperpolarised potentials. However, closer analysis shows that in contrast to heag2 currents, the heag1 currents appear slower because they are initially sigmoidal, with an initial lag in channel opening, but that the subsequent time course (i.e. $t_{20-80\%}$) is in fact faster for heag1 (Fig. 4C), at least for holding potentials in the range -100 mV to -60 mV. The voltage dependence of $t_{20-80\%}$ (Fig. 4C) is steeper for heag1 than for heag2, and shows saturation. Since the Cole–Moore shift is likely due to voltage-dependent shifts in occupation of two or more closed states, the transitions between closed states seem to be less voltage-sensitive for heag2 than for heag1.

Heag2 and heag1 currents were little affected by TEA, 1 mM, and partially blocked at 10 mM (Fig. 5A,B). The IC_{50} for both channels was somewhat greater than 10 mM (Fig. 5E). The fact that TEA can produce a block is consistent

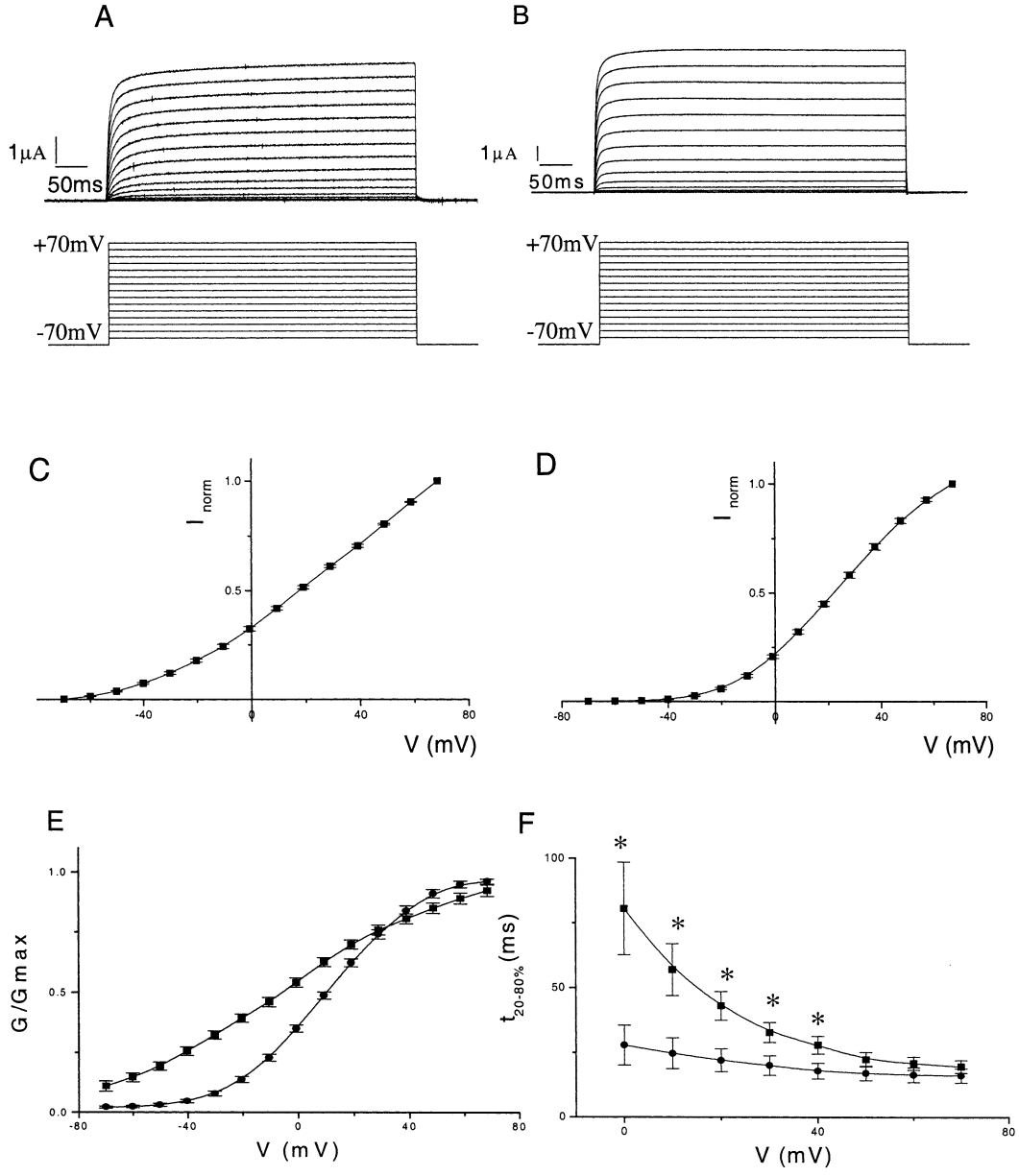

Fig. 3. Functional expression of heag2 and heag1 in oocytes. Examples of potassium currents are shown for heag2 (A) and heag1 (B) during a series of depolarising steps from −80 mV to the potentials shown. Mean normalised (I_{norm}) *I–V* curves are shown for heag2 (C) and heag1 (D) ($n = 17$–20). The corresponding conductance–voltage (*G–V*) curves are shown (E) for heag2 (■) and heag1 (●). The mean activation times, $t_{20-80\%}$, are shown (F) for heag2 (■) and heag1 (●); $^*P < 0.05$.

with the potassium channel nature of these proteins. The antihistamine terfenadine at 1 μM had no effect on heag currents, while 10 μM terfenadine produced inhibition (Fig. 5C,D). The extent of the block by terfenadine was significantly greater ($P < 0.05$) for heag1 than for heag2 (Fig. 5E); the IC_{50} for heag1 was about 10 μM.

4. Discussion

The heag2 channel is the eighth human channel of the ether-a-go-go family to be cloned, completing this family of genes in human. RNA for this channel was found in brain and skeletal muscle, as for heag1 [6,15], although it was also found at lower levels throughout a range of other tissues. The primary structural features and domains of the heag2 sequence are similar to those of heag1, except for a variable stretch in the C-terminal region (VD domain, Fig. 1). As for heag1, the heag2 channel is characterised by outward rectification without inactivation, and slow activation; the activation kinetics depend on holding potential.

The *G–V* curves showed that the voltage for half-maximal activation was shifted to the left for heag2 as compared with heag1, as also occurs for the rat eag channels [4]. The *G–V* curves were also steeper for heag1, reflecting steeper voltage sensitivity of channel opening. Furthermore, activation kinetics differed between the two channels, suggestive of steeper voltage sensitivity also between closed states for heag1. By analogy with other voltage-dependent ion channels, the S4 region is the voltage sensor [16], and so one might have expected differences in S4 between the two channels. However,

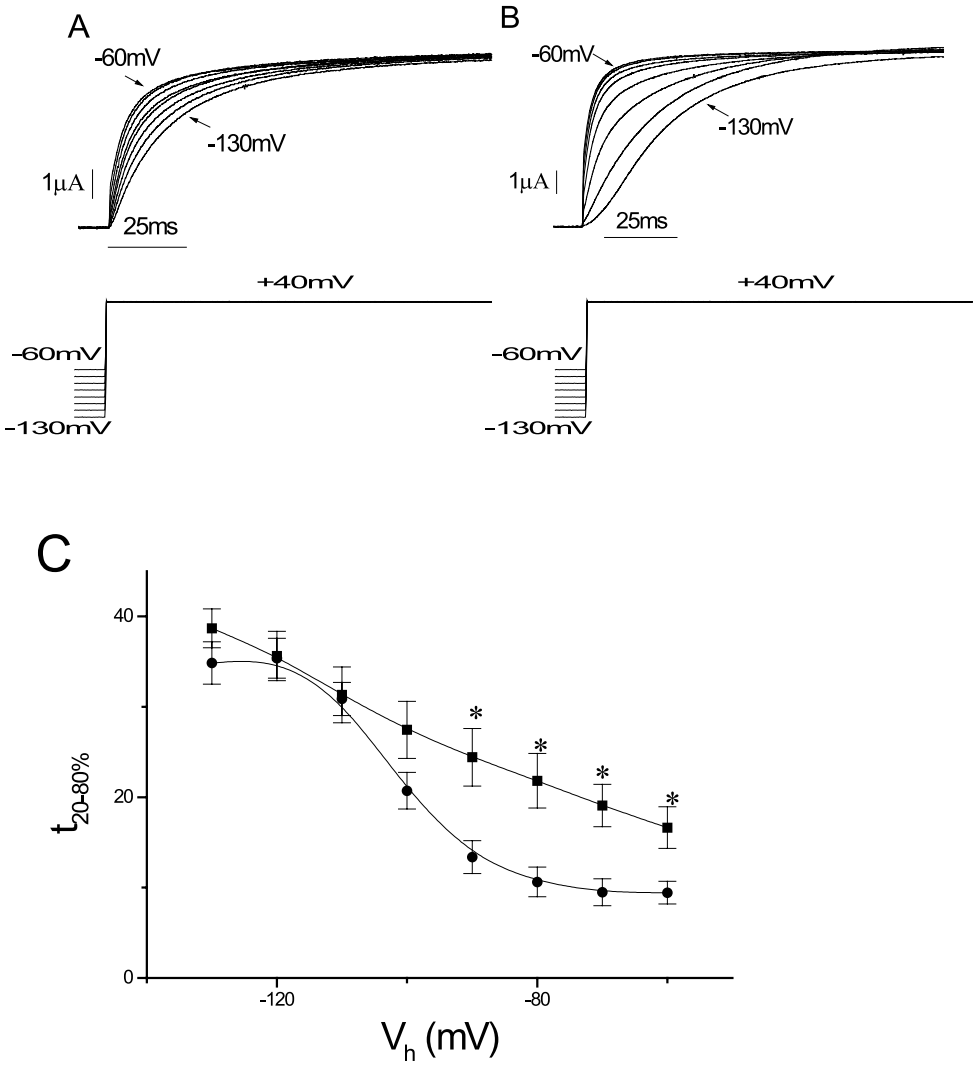

Fig. 4. Dependence of heag currents on holding potential. Examples of potassium currents for heag2 (A) and heag1 (B) are shown for depolarising steps to +40 mV from holding potentials of −130 mV to −60 mV. The corresponding activation times ($t_{20-80\%}$) are plotted (C) against holding potential, V_h, for heag2 (■) and heag1 (●), and the means are given for five to seven cells; $^*P < 0.05$.

the S4 region is identical between heag1 and heag2, and therefore other, as yet unknown, molecular regions of the protein must contribute to these differences in activation processes. Residues in the S4–S5 linker have already been implicated in deactivation kinetics for other channels in the ether-a-go-go family [17,18], but there is only one amino acid difference between heag1 and heag2 in this linker, and our mutational studies (unpublished data) have shown that this residue is not responsible for changes in *I–V* curves. Differences in activation properties are likely due to differences in the N- and/or C-terminal regions of these channels.

Both heag1 and heag2 channels were weakly sensitive to TEA, as already found for rat eag channels [4,5]. A range of compounds have been found to block herg channels, including class III antiarrhythmics, antihistamines, antibiotics, antipsychotics and gastrointestinal prokinetic drugs [19]. In the present paper, we showed that the antihistamine terfenadine blocked both heag1 and heag2 channels, although with greater sensitivity for heag1. The IC_{50} (around 10 μM) for heag1 is much larger than for herg channels (approx. 200 nM [20]). Although the corresponding pore-facing residues implicated in terfenadine block for herg [19] are identical to those in both heag1 and heag2, the extent of block is correlated with the extent of inactivation [21], which is marked for herg but absent for heag1 and heag2. Differences in sensitivity to blocking drugs between heag1 and heag2 are probably due to one or more of the seven amino acids that differ between heag1 and heag2 in the P and S6 regions, even though these may not face the pore, as also occurs for herg [22].

The physiological role of heag2 channels is currently unknown. However, the heag1 channel is implicated in cell cycle-specific myotube fusion [6], and interestingly heag2 was found in skeletal muscle. Furthermore, cell cycle-specific expression of eag1 has been shown to be important in cellular development and tumour growth [15,23], and a similar physiological role of heag2 in the cell cycle may also be of importance. The cellular location of heag1 and heag2 predominantly in the brain points to important physiological processes in brain function. The finding of heag2 in the heart was unexpected and deserves further investigation, but may perhaps be due to a non-functional splice variant (cf. $Herg_{USO}$ [13]).

After the present work was independently completed, an interesting paper [24] appeared which also reported the cloning and functional expression of heag2. The present paper

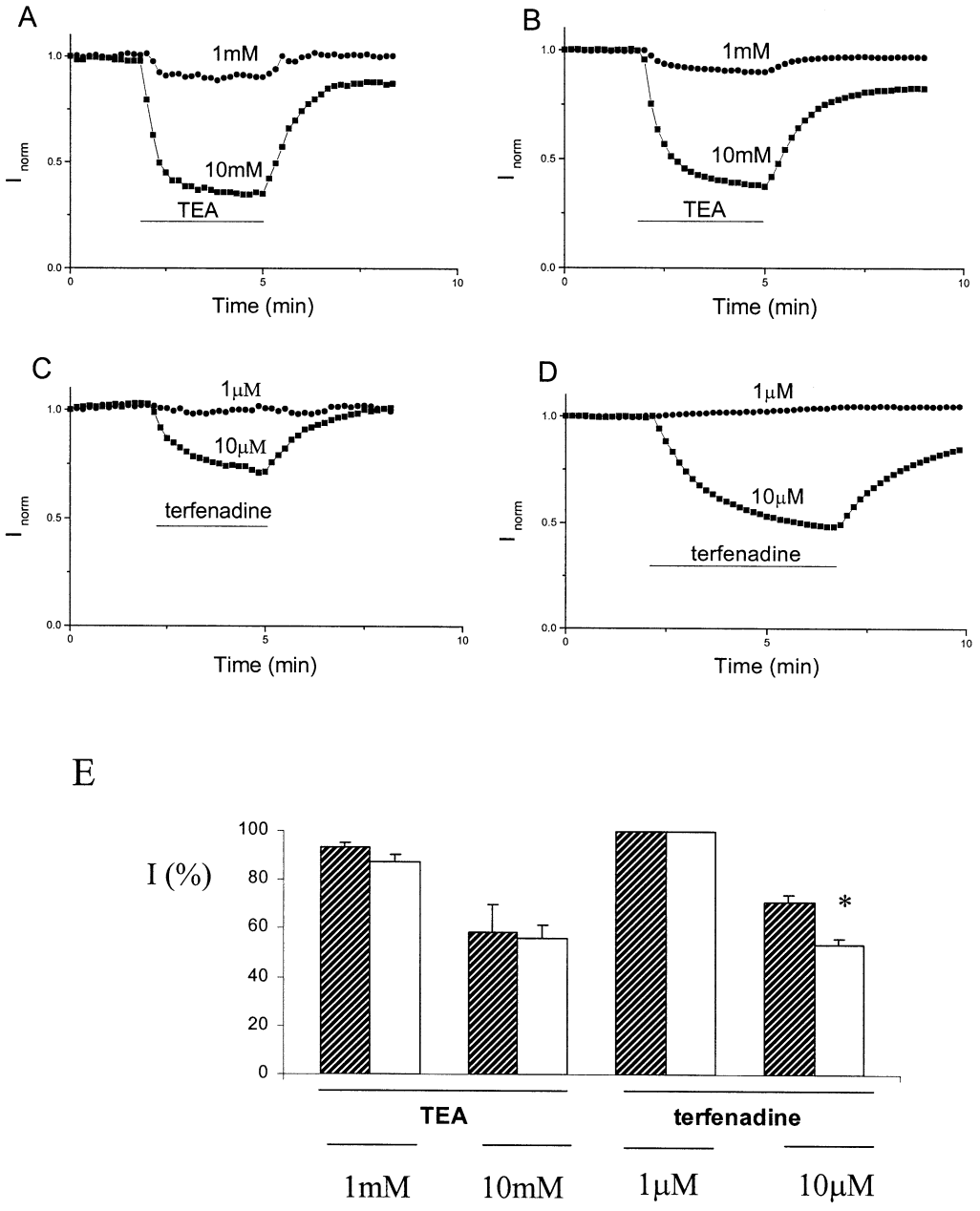

Fig. 5. Pharmacology of heag channels. TEA was applied during repetitive stimulation to +40 mV from a holding potential of −80 mV. Example recordings are shown for the application of TEA to heag2 (A) and heag1 (B) and for the application of terfenadine to heag2 (C) and heag1 (D). Drugs were applied during the period shown by the bar at the concentrations shown, followed by washing. Mean values are shown (E) for heag2 (shaded columns) and heag1 (unshaded) ($n = 3$ throughout, except for terfenadine at 1 μM, $n = 2$); $^*P < 0.05$.

provides new, complementary information as follows. Here we have studied and described the tissue distribution of heag2, in vitro translation, as well as the primary amino acid structural features as compared with heag2 (as well as a splice variant); these areas were not addressed by Schonherr et al. [24]. The present paper describes functional expression in oocytes, but our experiments were different in several respects from those in [24]. Thus for *I–V* curves we used physiological potassium solutions and activation studies rather than high potassium and deactivation studies. Although our results for the slope factor k of Boltzmann fits to the *G–V* curves were qualitatively similar to those of [24] (heag1 two times steeper than heag2), our results for $V_{0.5}$ were different. For $V_{0.5}$ we observed a shift to the left for heag2 as compared with heag1, consonant with results for rat eag channels [4], but differing from the rightwards shift reported in [24]. For the study of hyperpolarising voltages on the kinetics of activation, in contrast to [24], we carried out experiments in the absence of magnesium which of course itself affects kinetics, and we presented our results directly in terms of activation times rather than indirectly in terms of the model-dependent parameters used in [24]. Our data show the presence of the Cole–Moore shift for heag2 in the absence of magnesium, and suggest a steeper voltage sensitivity between closed states for heag1 than for heag2. We tested pharmacological blockers with oocytes rather than with mammalian cells used in [24], and we found a greater degree of block by TEA (10 mM) than in [24]. Terfenadine (not tested in [24]) showed lower sensitiv-

ity for heag2, qualitatively, though not quantitatively, similar to quinidine [24]. Finally, the clone described in [24] displays the A745T polymorphism which we have already referred to (see Section 3).

In summary, in this paper we have cloned and characterised the last member of the ether-a-go-go family, heag2, and compared its functional properties with heag1. It will be interesting to determine the reasons, at the molecular level, for the observed differences in functional properties between these two channels.

Acknowledgements: We would like to thank D. Gawler, L. Rashleigh and M. Al-Owais for their help.

References

[1] Wray, D. (2001) Pharm. News 8 (2), 12–17.
[2] Packer, J., Conley, E., Castle, N., Wray, D., January, C. and Patmore, L. (2000) Trends Pharmacol. Sci. 21, 327–328 (poster insert).
[3] Bauer, C.K. and Schwarz, J.R. (2001) J. Membr. Biol. 182, 1–15.
[4] Saganich, M.J., Vega-Saenz de Miera, E., Nadal, M.S., Baker, H., Coetzee, W.A. and Rudy, B. (1999) J. Neurosci. 19, 10789–10802.
[5] Ludwig, J., Weseloh, R., Karschin, C., Liu, Q., Netzer, R., Engeland, B., Stansfield, C. and Pongs, O. (2000) Mol. Cell. Neurosci. 16, 59–70.
[6] Occhiodoro, T., Bernheim, L., Liu, J-H., Bijlenga, P., Sinnreich, M., Bader, C.R. and Fischer-Lougheed, J. (1998) FEBS Lett. 434, 177–182.
[7] Milligan, C.J. and Wray, D. (2000) Biophys. J. 78, 1852–1861.
[8] Cabral, J.H.M., Lee, A., Cohen, S.L., Chait, B.T., Li, M. and Mackinnon, R. (1998) Cell 95, 649–655.
[9] Cui, J., Kagan, A., Qin, D., Mathew, J., Melman, Y.F. and McDonald, T.V. (2001) J. Biol. Chem. 276, 17244–17251.
[10] Ludwig, J., Owen, D. and Pongs, O. (1997) EMBO J. 16, 6337–6345.
[11] Schonherr, R., Lober, K. and Heinemann, S.H. (2000) EMBO J. 19, 3263–3271.
[12] Stansfield, C.E., Roper, J., Ludwig, J., Weseloh, R.M., Marsh, S.J., Brown, D.A. and Pongs, O. (1996) Proc. Natl. Acad. Sci. USA 93, 9910–9914.
[13] Kupershmidt, S., Snyder, D.J., Raes, A. and Roden, D.M. (1998) J. Biol. Chem. 273, 27231–27235.
[14] Ludwig, J., Terlau, H., Wunder, F., Bruggemann, A., Pardo, L.A., Marquardt, A., Stuhmer, W. and Pongs, O. (1994) EMBO J. 13, 4451–4458.
[15] Pardo, L.A., del Camino, D., Sanchez, A., Alves, F., Brugemann, A., Beckh, S. and Stuhmer, W. (1999) EMBO J. 18, 5540–5547.
[16] Wray, D. (2000) Sci. Spectra 23, 64–71.
[17] Sanguinetti, M.C. and Xu, Q.P. (1999) J. Physiol. 514, 667–675.
[18] Terlau, H., Heinemann, S.H., Stuhmer, W., Pongs, O. and Ludwig, J. (1997) J. Physiol. 502, 537–543.
[19] Mitcheson, J.S., Chen, J., Lin, M., Culberson, C. and Sanguinetti, C. (2000) Proc. Natl. Acad. Sci. USA 97, 12329–12333.
[20] Crumb, W.J. (2000) J. Pharmacol. Exp. Ther. 292, 261–264.
[21] Ficker, E., Jarolimek, W. and Brown, A.M. (2001) Mol. Pharmacol. 60, 1343–1348.
[22] Ishii, K., Kondo, K., Takahashi, M., Kimura, M. and Endoh, M. (2001) FEBS Lett. 506, 191–195.
[23] Camacho, J., Sanchez, A., Stuhmer, W. and Pardo, L.A. (2000) Pflugers Arch. 441, 167–174.
[24] Schonherr, R., Gessner, G., Lober, K. and Heinemann, S. (2002) FEBS Lett. 514, 204–208.